LA-UR-13-28479
Approved for public release; distribution is unlimited.

Title: Fast- and Slow- Mode Field Matching Across a Plasma Boundary

Author(s): Light, Max E.

Intended for: Report

Issued: 2013-11-05

Fast- and Slow- Mode Field Matching Across a Plasma Boundary

Max Light

October 30, 2013

Abstract

We determine how the amplitude and phase of each wave field component of an electromagnetic (EM) wave is split between the fast and slow roots of the cold plasma dispersion relation as it propagates across a plasma boundary.

Contents

1 Introduction

As an upward travelling EM wave encounters the underside of the ionosphere, each vectorial component of the wave's fields will be separated into two distinct parts due to the bi-refringent nature of the magnetized plasma in the ionosphere. Each part, or mode, may or may not propagate depending on the dispersive characteristics of the plasma at each frequency component of the incoming wave.

This mode partitioning comes from the four solutions of the Cold Plasma Dispersion Relation (CPDR): a forward and backward travelling *fast* wave root, and a forward and backward travelling *slow* wave root. These four roots come from the solution of the wave equation derived from the Maxwell equations, which is fourth order in a magnetized plasma. From now on, we will talk about the *two* principal roots (fast and slow), understanding that each has a forward and backward component.

Each mode has different dispersive characteristics, and will contribute differently to the amplitude and phase of each wave field component. Thus, in order to accurately track the wave as it propagates through the ionosphere, we must know how each wave field component is split between the fast and slow wave roots of the CPDR at the entrance and exit of the ionosphere. This information is critical in applications where EM radiation is propagated through the ionosphere and detected at a satellite-based antenna. For example, in ray tracing techniques, the amplitude and phase of the fast and slow wave modes is tracked separately through the ionosphere. Correct power partitioning between the modes is required to be able to superpose the transmitted fields at the receiver.

Our goal is to accurately partition the contribution of each mode in each wave field component (or *mode polarization*) as the wave encounters, traverses, and exits the ionospheric plasma. We explain the method of determining this partitioning assuming a smooth plasma transition, where the reflected wave field components are neglected; and also an abrupt transition where reflections are included.

For this report, we assume a cold, collisionless plasma in which the ions are too massive to respond to any phenomena on the time scale of the EM wave (RF frequency).

Figure 1 shows the general situation of EM propagation through the ionosphere. A signal is assumed to originate on the surface of the earth, or somewhere in the lower atmosphere. It then encounters the underside of

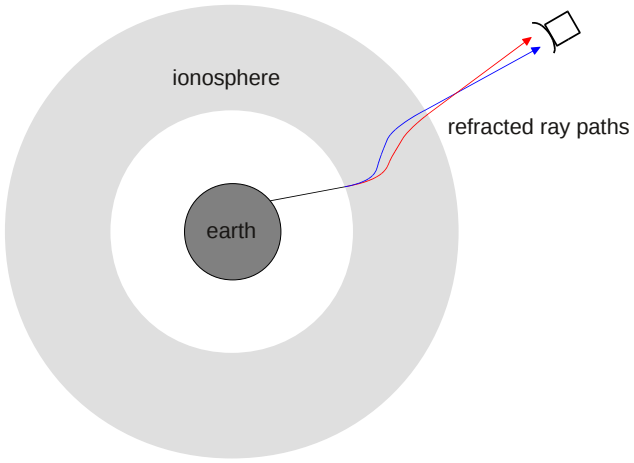

Figure 1: EM wave propagation through the ionosphere represented by rays. The ionosphere introduces a bi-refringent mode splitting of the incident wave.

the ionosphere and undergoes a bi-refringent mode splitting inside the magnetized ionospheric plasma. Each mode will then propagate through the ionosphere suffering different dispersive characteristics (sometimes only one or neither will traverse the whole ionospheric width at a given frequency), and then emerge on the topside, where the total electric field can then be calculated as the superposition of each mode contribution to each wave field component. Figure 2 shows the same situation, focusing on the point where the wave first encounters the ionosphere. In general, the wave will undergo reflection and refraction at the boundary, with both parts being partitioned into fast and slow mode components. In order to characterize the partitioning of each mode component for the refracted (and reflected) parts, it is first necessary to decompose the incident EM wave into these components, which can then be followed across the boundary. This means that we must be able to partition the mode contributions of the incident EM wave fields *in vacuum* prior to crossing the initial plasma boundary. Basically, we need to solve for the vacuum EM wave fields using the CPDR for a zero density plasma. In order to continue with the calculation of the wave fields' mode polarizations, then, we need to summarize the main points in the derivation and solution of the CPDR.

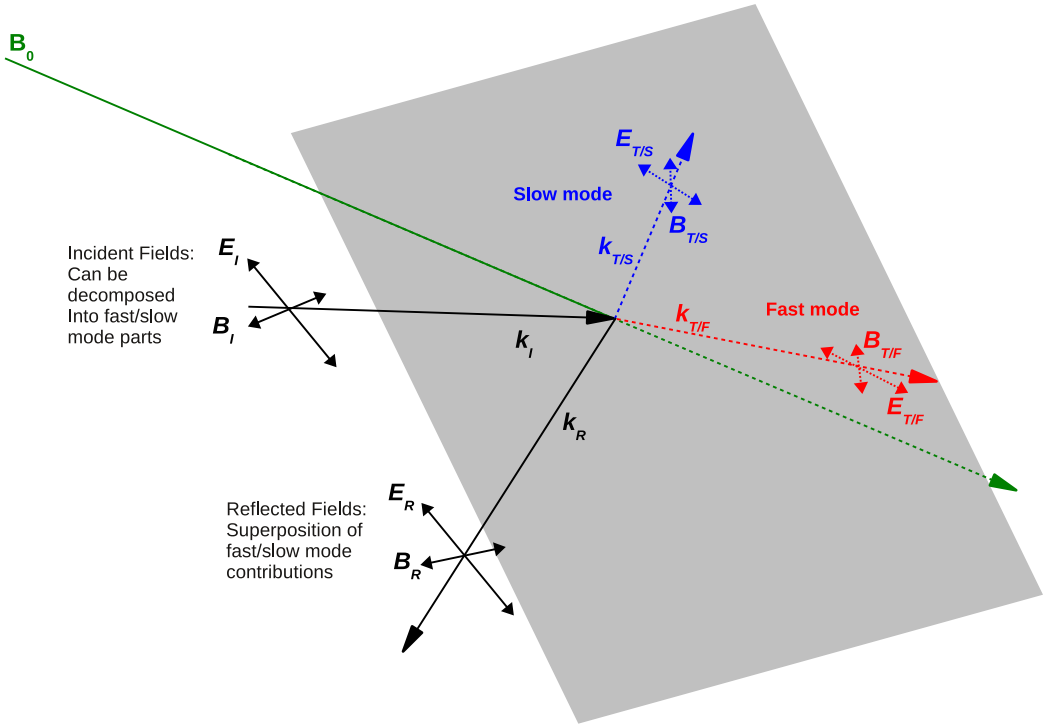

Figure 2: EM wave interaction at a plasma boundary. The plasma boundary has an oblique orientation to the magnetic field $\mathbf{B_0}$ and the incident wave $\boldsymbol{k_i}$.

2 Cold plasma dispersion relation (CPDR)

2.1 Derivation

In this section, we will assume that the CPDR is found in the local coordinate system of the plasma, and we will choose to let $\mathbf{B_0}$ lie along one of the principal axes (z). We will draw heavily from standard texts by Swanson [8], Budden [2], Kraus [6], and Allis et. al. [1]. Vector quantities are bold.

We assume a time harmonic form for the fields, that is

$$\boldsymbol{E}(\boldsymbol{r},t) = \boldsymbol{E}(\boldsymbol{r})e^{-i\omega t} \qquad \boldsymbol{H}(\boldsymbol{r},t) = \boldsymbol{H}(\boldsymbol{r})e^{-i\omega t} \tag{1}$$

where $\boldsymbol{E}(\boldsymbol{r}), \boldsymbol{H}(\boldsymbol{r})$ are complex valued. We also assume a plane wave spatial

structure for the propagating EM signals considered in this report. This is accurate given that we are concerned with the VHF band of frequencies propagating in the ionosphere. These assumptions give the final form of the fields as

$$\boldsymbol{E}(\boldsymbol{r},t) = E_0 e^{i(\boldsymbol{k}\cdot\boldsymbol{r}-\omega t)} \qquad \boldsymbol{H}(\boldsymbol{r},t) = H_0 e^{i(\boldsymbol{k}\cdot\boldsymbol{r}-\omega t)} \tag{2}$$

The electric field wave equation inside the plasma is

$$\mathbf{n}\times\mathbf{n}\times\mathbf{E} + \overline{\epsilon_{\mathbf{r}}}\cdot\mathbf{E} = 0 \tag{3}$$

with $\mathbf{n}$ defined as the index of refraction

$$\mathbf{n} = \frac{c}{\omega}\mathbf{k} \tag{4}$$

$\overline{\epsilon_{\mathbf{r}}}$ is the plasma dielectric tensor, whose elements we will leave in a general form for now

$$\overline{\epsilon_{\mathbf{r}}} = \begin{pmatrix} \epsilon_{11} & \epsilon_{12} & \epsilon_{13} \\ \epsilon_{21} & \epsilon_{22} & \epsilon_{23} \\ \epsilon_{31} & \epsilon_{32} & \epsilon_{33} \end{pmatrix} \tag{5}$$

This tensor is, in general, not Hermitian (for instance, when collisional effects are included); where a Hermitian matrix has the property (* denotes complex conjugate)

$$\epsilon_{ij} = \epsilon_{ji}^* \tag{6}$$

However, it does have Onsager symmetry, that is

$$\epsilon_{ij}(B_0) = \epsilon_{ji}(-B_0) \qquad (\omega_c \to -\omega_c) \tag{7}$$

where B_0 is the magnetic field and ω_c is the electron cyclotron frequency.

Equation 3 is

$$\overline{\mathbf{K}}\cdot\mathbf{E} = 0 \tag{8}$$

which, in matrix form is given as

$$\begin{pmatrix} \epsilon_{11}-(n_y^2+n_z^2) & \epsilon_{12}+n_xn_y & \epsilon_{13}+n_xn_z \\ \epsilon_{21}+n_xn_y & \epsilon_{22}-(n_x^2+n_z^2) & \epsilon_{23}+n_yn_z \\ \epsilon_{31}+n_xn_z & \epsilon_{32}+n_yn_z & \epsilon_{33}-(n_x^2+n_y^2) \end{pmatrix} \begin{pmatrix} E_x \\ E_y \\ E_z \end{pmatrix} = 0 \tag{9}$$

This set of equations will have a non-trivial solution only if the determinant of the matrix goes to zero

$$\det\left|\overline{\mathbf{K}}\right| = G(\mathbf{k},\omega,\mathbf{r},t) = 0$$

or

$$\begin{vmatrix} \epsilon_{11} - (n_y^2 + n_z^2) & \epsilon_{12} + n_x n_y & \epsilon_{13} + n_x n_z \\ \epsilon_{21} + n_x n_y & \epsilon_{22} - (n_x^2 + n_z^2) & \epsilon_{23} + n_y n_z \\ \epsilon_{31} + n_x n_z & \epsilon_{32} + n_y n_z & \epsilon_{33} - (n_x^2 + n_y^2) \end{vmatrix} = 0 \tag{10}$$

The CPDR can, in general, be quite complicated depending on how the dielectric tensor matrix $\overline{\epsilon_{\mathbf{r}}}$ is populated. We know that wave propagation in a cold, collisionless, magnetized plasma is affected by the anisotropy introduced by the magnetic field such that the wave propagation is only dependent on its direction relative to this field. In other words, a potentially three dimensional system is reduced to a two dimensional system because the principle directions of wave propagation are *along* and *across* $\mathbf{B_0}$. Mathematically, this means that we are always free to rotate a magnetized plasma system to one in which the principle axes are along and across $\mathbf{B_0}$ such that $\boldsymbol{k}$ and $\mathbf{B_0}$ are *co-planar*.

Thus, we choose $\mathbf{B_0}$ to lie along the z axis and $\boldsymbol{k}$ to lie in the x-z plane in a 2-D coordinate system, shown in Fig. 3. This is a system with rotational

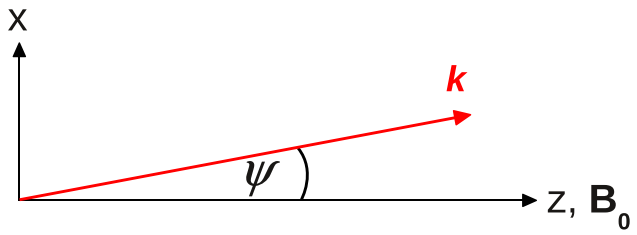

Figure 3: Orientation for solution to the CPDR.

symmetry about the z axis - we can always pick a coordinate system where the wave propagation properties in a magnetized plasma are completely described in a two dimensional manner. therefore, the y-component of the wave number, k_y, (or refractive index n_y) in the rectilinear version of this system (or k_ϕ, n_ϕ in a cylindrical geometry) can be ignored. The plasma dielectric tensor in this system reduces to

$$\overline{\epsilon_{\mathbf{r}}} = \begin{pmatrix} S & -iD & 0 \\ iD & S & 0 \\ 0 & 0 & P \end{pmatrix} \tag{11}$$

whose elements are

$$\begin{aligned} S &= 1 - \frac{X}{1-Y^2} \\ D &= \frac{-XY}{1-Y^2} \\ P &= 1 - X \end{aligned} \tag{12}$$

with X and Y defined in the usual way for the ionospheric physics community

$$X = \omega_p^2/\omega^2 \qquad Y = \omega_c/\omega \tag{13}$$

From equation 10, setting the determinant of $\overline{\mathbf{K}}$ to zero (neglecting n_y, as outlined earlier) will give the CPDR as a quadratic in $n^2 = |\mathbf{n}|^2$ as

$$An^4 - Bn^2 + C = 0 \tag{14}$$

where

$$\begin{aligned} A &= S\sin^2\psi + P\cos^2\psi \\ B &= (S^2 - D^2)\sin^2\psi + PS(1+\cos^2\psi) \\ C &= P(S^2 - D^2) \end{aligned} \tag{15}$$

The solution to this polynomial equation is written in the standard form

$$n_\pm^2 = \frac{B \pm \sqrt{B^2 - 4AC}}{2A} \tag{16}$$

n_+ and n_- are identified as the *slow*- and *fast*- wave roots of the CPDR; 'slow' and 'fast' referring to the phase velocity of one wave relative to the other. These two root branches determine the mode splitting of an EM wave as it traverses the ionosphere.

Note that it is the presence of $\mathbf{B_0}$ that causes the bi-refringent nature of the ionosphere: the two solutions to equation 16 representing the two possible wave number solutions for propagation. To demonstrate this, set $\mathbf{B_0} = 0$ in

equations 12. Since we specify $\mathbf{B_0} \to 0$, there is no longer an anisotropy in the plasma and we are free to choose $\psi \to 0$ as well. The plasma dielectric tensor reduces to a scalar

$$\overline{\epsilon_{\mathbf{r}}} \to \begin{pmatrix} P & 0 & 0 \\ 0 & P & 0 \\ 0 & 0 & P \end{pmatrix} \to \epsilon_r = P = 1 - X \tag{17}$$

The CPDR only has one principal root in this case (see equation 10) given by the familiar CPDR for an unmagnetized plasma

$$\begin{aligned} n^2 &= 1 - X \\ n &= \pm\sqrt{1 - \omega_p^2/\omega^2} \end{aligned} \tag{18}$$

Turning back to a magnetized plasma system, the well known Appleton-Hartree dispersion relation (AHDR) for a cold, collisionless plasma is [2]

$$n^2 = 1 - \frac{X(1-X)}{1 - X - \frac{1}{2}Y^2\sin^2\psi \pm \left[\frac{1}{4}Y^4\sin^4\psi + Y^2\cos^2\psi(1-X)^2\right]^{1/2}} \tag{19}$$

which appears to be quite different from the CPDR given in equations 14 to 16, and they were, in fact, derived in slightly different coordinate systems (ours with $\mathbf{B_0} \parallel z$ and AHDR with $\boldsymbol{k} \parallel z$, both cases have $\boldsymbol{k} \cdot \mathbf{B_0} = |\boldsymbol{k}||\mathbf{B_0}|\cos\psi$). However, the symmetry of wave propagation in a magnetized plasma and the invariance of 3×3 matrix determinants to 1, 2, or 3 axis rotations (coordinate transformations) means that these dispersion relations for n^2 are *equivalent*, while the individual components of $\mathbf{n}$ (n_i, n_j, n_k where i, j, k represent the coordinate axes and $n = [n_i^2 + n_j^2 + n_k^2]^{1/2}$) will have different relative values.

2.2 Coordinate transformations for solving the CPDR

Our solution of the CPDR in the previous section relied on the rotational symmetry inherent in a magnetized plasma system. For a wave travelling obliquely through a magnetized plasma, we have the choice of either transforming the reference frame to the *symmetric* coordinate system, where the plasma dielectric tensor is given from equation 11, or solving for the fields in

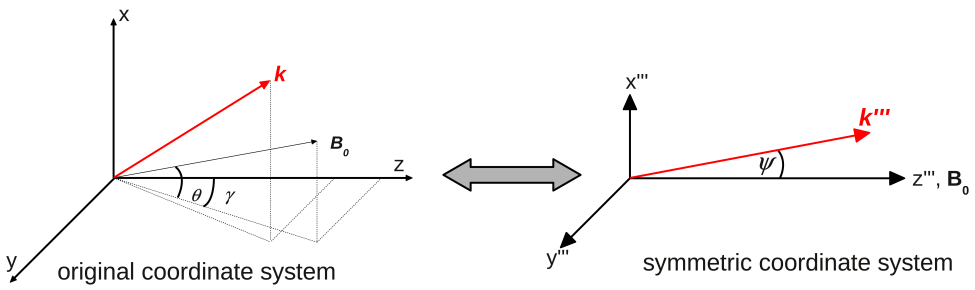

Figure 4: Coordinate transform for solution of the CPDR.

the *original* coordinate system with the plasma dielectric tensor rotated into this system. These coordinate systems are illustrated in Fig. 4.

In the symmetric coordinate system, all field quantities are rotated into this system and the dielectric tensor of equation 11 is employed. The wave equation is

$$\mathbf{n}''' \times \mathbf{n}''' \times \mathbf{E}''' + \overline{\epsilon_\mathbf{r}} \cdot \mathbf{E}''' = 0 \tag{20}$$

where the superscript $(''')$ signifies that the field quantities are transformed (rotated) from the original system, for example

$$\mathbf{n}''' = \overline{\mathbf{R}} \cdot \mathbf{n} \tag{21}$$

and $\overline{\mathbf{R}}$ is the appropriate coordinate rotation matrix.

In the original coordinate system, the field quantities are not transformed, but the plasma dielectric tensor (which was originally derived in the symmetric coordinate system) must be transformed. The wave equation is then

$$\mathbf{n} \times \mathbf{n} \times \mathbf{E} + \overline{\epsilon'''_\mathbf{r}} \cdot \mathbf{E} = 0 \tag{22}$$

where $\overline{\epsilon'''_\mathbf{r}}$ is the plasma dielectric tensor rotated from the symmetric coordinate system using the coordinate transformation properties of tensors and the appropriate coordinate transformation matrix $\overline{\mathbf{R}}$

$$\overline{\epsilon'''_\mathbf{r}} = \overline{\mathbf{R}}^\mathbf{T} \cdot \overline{\epsilon_\mathbf{r}} \cdot \overline{\mathbf{R}} \tag{23}$$

The superscript $(^T)$ corresponds to the matrix transpose. Coordinate transformation matrices are orthogonal by definition, whereupon their transpose is the same as their inverse.

2.2.1 Transforming fields to the symmetric coordinate system

We will do this by requiring that $k_y \rightarrow 0$ in the new coordinate system and assuming that the magnetic field angles θ and γ in Fig. 4 are known. We want to rotate the coordinate system such that $\mathbf{B_0}||\boldsymbol{z}$ and the transformed wave number $\boldsymbol{k'''}$ and $\mathbf{B_0}$ are in the x-z plane. This will be accomplished through three coordinate axis rotations, as described below. For each rotation, a prime (') will be added to the coordinate and vector names for clarity. After the three coordinate rotations, $\mathbf{B_0}$ will make an angle ψ with the z''' axis.

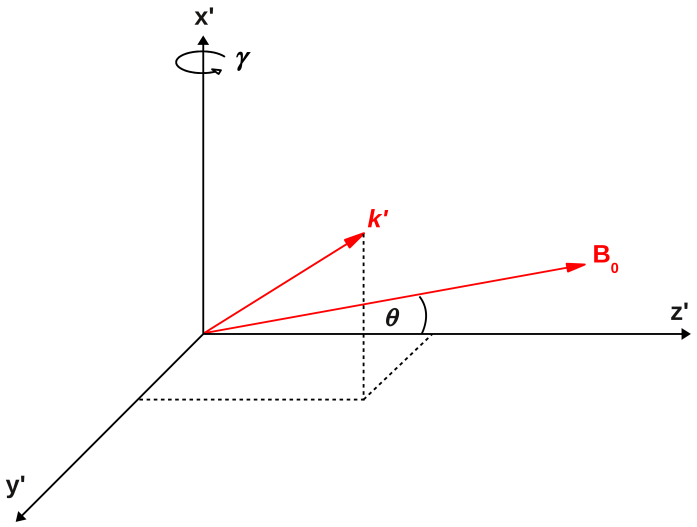

Figure 5: The first coordinate rotation about the x axis. This shows the situation *after* the rotation.

First coordinate rotation: $\boldsymbol{x}$ axis We first rotate about the x-axis by an angle γ to make $\mathbf{B_0}$ and $\boldsymbol{z'}$ co-planar (after rotation). This is illustrated in Fig 5. We use the standard three dimensional axis rotation matrix such that

$$\begin{pmatrix} k_x{}' \\ k_y{}' \\ k_z{}' \end{pmatrix} = \overline{\mathbf{R}}_{\mathbf{x}\gamma} \begin{pmatrix} k_x \\ k_y \\ k_z \end{pmatrix} \tag{24}$$

where the rotation about $\boldsymbol{x}$ is given by

$$\overline{\mathbf{R}}_{\mathbf{x}\gamma} = \begin{pmatrix} 1 & 0 & 0 \\ 0 & \cos\gamma & \sin\gamma \\ 0 & -\sin\gamma & \cos\gamma \end{pmatrix} \tag{25}$$

Second coordinate rotation: $\boldsymbol{y}^{'}$ axis Next, rotate about the $y^{'}$-axis by an angle θ to place $\mathbf{B_0}$ along the $z^{''}$-axis using $\overline{\mathbf{R}_{\mathbf{y}\theta}}$, as shown in Fig. 6

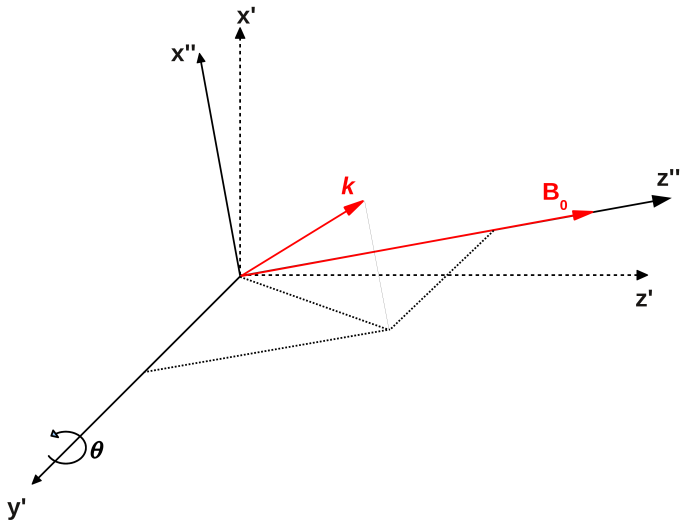

Figure 6: The second coordinate rotation about the $y^{'}$ axis.

$$\begin{pmatrix} k_x^{''} \\ k_y^{''} \\ k_z^{''} \end{pmatrix} = \begin{pmatrix} \cos\theta & 0 & -\sin\theta \\ 0 & 1 & 0 \\ \sin\theta & 0 & \cos\theta \end{pmatrix} \begin{pmatrix} k_x^{'} \\ k_y^{'} \\ k_z^{'} \end{pmatrix} \tag{26}$$

Third coordinate rotation: $\boldsymbol{z}^{''}$ axis Finally, as shown in Fig. 7, we rotate about the $z^{''}$-axis by an angle α so that $\boldsymbol{k}_{\boldsymbol{y}}^{'''} \rightarrow 0$ using $\overline{\mathbf{R}}_{\mathbf{z}\alpha}$. After this rotation, $\boldsymbol{k}$ will have an angle ψ with respect to $\mathbf{B_0}$ given by

$$\psi = \arctan \frac{k_x^{'''}}{k_z^{'''}} \tag{27}$$

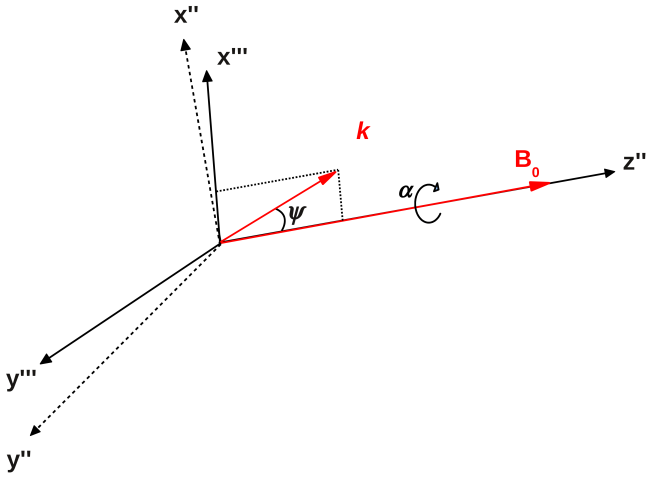

Figure 7: The third coordinate rotation about the z'' axis.

$$\begin{pmatrix} k_x''' \\ 0 \\ k_z''' \end{pmatrix} = \begin{pmatrix} \cos\alpha & \sin\alpha & 0 \\ -\sin\alpha & \cos\alpha & 0 \\ 0 & 0 & 1 \end{pmatrix} \begin{pmatrix} k_x'' \\ k_y'' \\ k_z'' \end{pmatrix} \tag{28}$$

We find the rotation angle α from the middle equation of 28 in terms of the known angles γ and θ, and the wave number components k_x, k_y, and k_z:

$$\alpha = \arctan\left(\frac{k_z \sin\gamma + k_y \cos\gamma}{k_x \cos\theta - k_z \cos\gamma \sin\theta + k_y \sin\gamma \sin\theta}\right) \tag{29}$$

The symmetric coordinate system in which $k_y''' \rightarrow 0$ is now completely specified. We can transform fields from original to symmetric coordinate systems using the three rotation matrices specified above. For example, the electric fields are transformed using

$$\begin{pmatrix} E_x''' \\ E_y''' \\ E_z''' \end{pmatrix} = \overline{\mathbf{R}} \begin{pmatrix} E_x \\ E_y \\ E_z \end{pmatrix} \tag{30}$$

where

$$\overline{\mathbf{R}} = \overline{\mathbf{R}}_{\mathbf{z}\alpha}\, \overline{\mathbf{R}}_{\mathbf{y}\theta}\, \overline{\mathbf{R}}_{\mathbf{x}\gamma} \tag{31}$$

To transform from symmetric back to the original coordinates, we simply left multiply by the inverse of the matrix formed by the product of the three rotation matrices

$$\begin{pmatrix} E_x \\ E_y \\ E_z \end{pmatrix} = \overline{\mathbf{R}}^{-1} \begin{pmatrix} E'''_x \\ E'''_y \\ E'''_z \end{pmatrix} \tag{32}$$

2.2.2 Transforming the plasma dielectric tensor into the original coordinate system

Here, we work in the original coordinate system, and transform the plasma dielectric tensor from the symmetric coordinate system into this one. The tensor transform is given by equations 23 and the rotation matrices in equations 25 and 26. Note that in this coordinate system, we need only *two* coordinate transformations. The magnetic field of the symmetric coordinate system only needs to be rotated about the x-axis by γ, and the y-axis by θ.

$$\overline{\epsilon'''_{\mathbf{r}}} = \overline{\mathbf{R}}^{\mathbf{T}} \cdot \overline{\epsilon_{\mathbf{r}}} \cdot \overline{\mathbf{R}} \tag{33}$$

where now the rotation matrix $\overline{\mathbf{R}}$ is given by

$$\overline{\mathbf{R}} = \overline{\mathbf{R}}_{\mathbf{x}\gamma}\, \overline{\mathbf{R}}_{\mathbf{y}\theta} = \begin{pmatrix} \cos\theta & \sin\gamma\sin\theta & -\cos\gamma\sin\theta \\ 0 & \cos\gamma & \sin\gamma \\ \sin\theta & -\cos\theta\sin\gamma & \cos\gamma\cos\theta \end{pmatrix} \tag{34}$$

And we write for convenience the transpose of the rotation matrix

$$\overline{\mathbf{R}}^{\mathbf{T}} = \begin{pmatrix} \cos\theta & 0 & \sin\theta \\ \sin\gamma\sin\theta & \cos\gamma & -\cos\theta\sin\gamma \\ -\cos\gamma\sin\theta & \sin\gamma & \cos\gamma\cos\theta \end{pmatrix} \tag{35}$$

3 Mode decomposition of incident EM wave vacuum fields

We now look to decompose the incident vacuum EM wave fields into fast and slow components, that is

$$\begin{aligned} \boldsymbol{E_i} &= \boldsymbol{E_i^{fast}} + \boldsymbol{E_i^{slow}} \\ &= \hat{x}\left(E_{xi}^{fast} + E_{xi}^{slow}\right) + \hat{y}\left(E_{yi}^{fast} + E_{yi}^{slow}\right) + \hat{z}\left(E_{zi}^{fast} + E_{zi}^{slow}\right) \end{aligned} \tag{36}$$

so that each mode component of each *vector part* can be propagated across the boundary correctly. In order to solve for the individual mode components, we must solve the CPDR in vacuum ($n_e \rightarrow 0 \Rightarrow X \rightarrow 0$), and look at the ratio of the field vector parts for each mode.

We will then construct a *mode polarization unit vector* $\hat{\boldsymbol{Q}}$ which represents the partitioning of the fast and slow mode contributions to each vector part of the incident EM wave field. Once we know how each vector part of the incident EM wave field is partitioned, we can correctly solve for the propagation characteristics of the EM wave without using any approximations on the amount of power in each mode. We must know the partitioning between fast and slow modes *before* any propagation algorithm is started for correct results.

3.1 E-field cofactor ratios

Assume that we have transformed all field quantities into the symmetric coordinate system, and that the plasma geometry is given by Fig 3. In this geometry, equation 9 is

$$\begin{pmatrix} S - n^2\cos^2\psi & -iD & n^2\cos\psi\sin\psi \\ iD & S - n^2 & 0 \\ n^2\cos\psi\sin\psi & 0 & P - n^2\cos^2\psi \end{pmatrix} \begin{pmatrix} E_x \\ E_y \\ E_z \end{pmatrix} = 0 \tag{37}$$

where the dispersion relation is is defined as choosing the index of refraction, n^2, such that the determinant of the 3×3 matrix is 0, that is, from equation 19

$$n^2 = 1 - \frac{X(1-X)}{1 - X - \frac{1}{2}Y^2\sin^2\psi \pm \left[\frac{1}{4}Y^4\sin^4\psi + Y^2\cos^2\psi(1-X)^2\right]^{1/2}} \tag{38}$$

and the slow/fast modes are determined from the $\pm$ in the denominator.

We can observe the E-field polarization characteristics by taking the E-field co-factor ratios in equation 37.

$$\begin{aligned} \frac{E_x}{E_y} &= i\frac{S - n^2}{D} \\ \frac{E_z}{E_y} &= \frac{(S - n^2)(n^2\cos\psi\sin\psi)}{iD(P - n^2\sin^2\psi)} \end{aligned} \tag{39}$$

where we have chosen to take the E-field cofactor ratios relative to E_y. We could have chosen any of the three vector components. Note that the index of refraction, n, appears as n^2 in the above ratios, and will have two solutions; a fast and slow root. Thus, we now have a foundation for finding the mode contribution to the EM wave fields.

3.2 Mode polarization unit vector construction

To continue, we solve the ratios in equation 39 in the limit $X \to 0$

$$\begin{aligned}
\lim_{X\to 0}\left(\frac{E_x}{E_y}\right) &= i\left[\frac{Y\sin^2\psi}{2}\left(1 \pm \left[1+\frac{4\cos^2\psi}{Y^2\sin^4\psi}\right]^{1/2}\right)\right] \\
\lim_{X\to 0}\left(\frac{E_z}{E_y}\right) &= i\left[\frac{Y\sin^2\psi}{2}\left(1 \pm \left[1+\frac{4\cos^2\psi}{Y^2\sin^4\psi}\right]^{1/2}\right)\right] \times \\
&\qquad \frac{(1+\cos^2\psi)\cos\psi\sin\psi}{(1+\cos^2\psi)\sin^2\psi - 2}
\end{aligned} \tag{40}$$

We can then construct a unit vector from these E-field cofactor ratios in this limit which represents the normalized amplitude of each mode to each vector wave part

$$\hat{\boldsymbol{Q}}^{\boldsymbol{F/S}} = \frac{\hat{\boldsymbol{x}}\lim_{X\to 0}\left(\frac{E_x}{E_y}\right)_{F/S} + 1\hat{\boldsymbol{y}} + \hat{\boldsymbol{z}}\lim_{X\to 0}\left(\frac{E_z}{E_y}\right)_{F/S}}{\sqrt{\left[\lim_{X\to 0}\left(\frac{E_x}{E_y}\right)_{F/S}\right]^2 + 1 + \left[\lim_{X\to 0}\left(\frac{E_z}{E_y}\right)_{F/S}\right]^2}} \tag{41}$$

We can now find the fast and slow mode contributions to the incident EM wave field vectorial components (in the symmetric coordinate system). They can be transformed into the desired coordinate system and used in an appropriate propagation algorithm. In the *symmetric* coordinate system, the individual mode components are found from the dot product of the mode component of $\hat{\boldsymbol{Q}}$ and the incident EM wave field vector

$$\begin{aligned}
\boldsymbol{E_{inc}}\cdot\hat{\boldsymbol{Q}}^{\boldsymbol{F}}\Big|_j &= E^F_{j,inc} \\
\boldsymbol{E_{inc}}\cdot\hat{\boldsymbol{Q}}^{\boldsymbol{S}}\Big|_j &= E^S_{j,inc}
\end{aligned} \tag{42}$$

where $j = x, y, z$.

We can also solve $\hat{\boldsymbol{Q}}^{\boldsymbol{F/S}}$ in the vacuum coordinate system using Eqns. 33, 34, and 35 in Eq. 22 and solving the respective field cofactor ratios for each mode.

4 EM Wave propagation and boundaries

As the EM wave passes from one medium to the next, its reflective and refractive properties will change. This is usually treated by either assuming an abrupt transition, where those properties change over an infinitesimally small length such as a vacuum/dielectric interface, or a smooth transition, where they change gradually over an unspecified characteristic length. Each assumption has advantages and disadvantages depending on the nature of the propagation characteristic to examine, the EM wave frequency, and characteristic transition length. For an EM wave incident on the ionosphere, we can quantify the difference between the two extremes in terms of the scale length over which any gradients in the plasma exist.

In a real-world situation, the ionosphere has a 'smooth' transition from vacuum to plasma, and back again. However, from the perspective of the incident EM wave, it's not enough to simply employ this assumption. If the wavelength of the EM radiation is much smaller than any ionospheric plasma gradients, for instance in the electron density or background magnetic field, then the wave will effectively sample a uniform background plasma over distances larger than a wavelength. On the other hand, an EM wave propagating from one medium to another that experiences plasma gradients over distances much smaller than the wavelength will see the background change significantly in a fraction of a wavelength. In either case, the change in background plasma parameters will affect the solution of the local CPDR, which will concomitantly change the wavelength. These two situations illustrate a demarcation between strategies for solving the wave fields. In one, we can invoke the well known WKB approximation outlined below, that is when the change of wavelength over a wavelength is *small*

$$\left| \frac{1}{k} \frac{dk}{dx} \right| \ll k \tag{43}$$

where x is a spatial coordinate along the gradient. When this is not true, we must use a different method. Intuitively, then, this illustrates the difference in a smooth versus abrupt transition for the EM wave.

4.1 Smooth boundary

For a smooth boundary, we assume the plasma changes over scale lengths much greater than the wavelength, and we can invoke the WKB approximation [8, 7, 5] . Under this approximation, the EM wave is treated using geometric optics wherein its trajectory and amplitude are found from the well known ray tracing technique. In this technique, the ray equations determine the trajectory of the ray, or group velocity vector, as it propagates through the ionospheric plasma

$$\begin{aligned} \frac{d\boldsymbol{k}}{d\tau} &= \frac{dG}{d\boldsymbol{r}} \\ \frac{d\boldsymbol{r}}{d\tau} &= -\frac{dG}{d\boldsymbol{k}} \\ \frac{d\omega}{d\tau} &= -\frac{dG}{dt} \end{aligned} \tag{44}$$

with the dispersion relation found from equation 10

$$G(\boldsymbol{k}, \omega, \boldsymbol{r}, t) = 0 \tag{45}$$

In this formalism, the amplitude of the ray along its trajectory is found from a separate set of equations [8, 7], by tracking 'bundles' of rays and observing their cross sectional spread with distance, or simply by dividing the initial amplitude by the distance along the ray path. Solution of the amplitude equations is significantly more difficult than the ray equations, and for that reason the latter two methods are usually employed.

Reflections due to media changes are higher order in the ray tracing technique and usually ignored. Furthermore, if the wave encounters a local cutoff or resonance, that is $k \to 0$ or $k \to \infty$, then this method will break down, and the wave field solution in this region must be found using alternative methods. So, even though the wavelength may change slowly, it can still approach a cutoff or resonance which will invalidate the ray tracing solution at those local points, and care must be used to guide the field solutions through these regions.

4.1.1 Smooth boundary - propagation implications

We can track the fields as they traverse the plasma under this formalism with a priori knowledge of the mode content of each field vectorial component,

which we can find with the help of the mode polarization unit vector $\hat{\boldsymbol{Q}}^{\boldsymbol{F/S}}$. Once this is solved, the fields can be propagated through the plasma using the ray tracing technique in the absence of reflections. Once the topside is reached, the individual field mode components are superposed and the total field is then propagated to the receiver. Reflection loss, as described above, is neglected in this approach.

4.2 Abrupt boundary

Abrupt boundary transitions are best illustrated by the classic problem of an EM wave incident on a dielectric half-space [5], where it undergoes reflection and refraction at the interface. These characteristics are found directly by solving for the transmission, T, and reflection, Γ, coefficients at the interface. It is important to note that reflections, which are usually ignored in the ray tracing technique, can be quite significant depending on the plasma gradient structure and EM wave frequency.

4.2.1 Abrupt boundary - propagation implications

In order to account for reflections, we must consider an abrupt plasma boundary, effectively squeezing down the transition thickness to be infinitesimally small. To propagate the EM wave through this layered ionosphere, we can choose to approach the layers as follows:

Single layer plasma with gradient Under this assumption, we solve for the reflection losses at the entrance and exit of the ionosphere, and propagate the individual modes under the ray tracing approximation through a single layer - which can be assumed to be homogeneous or inhomogeneous depending on the desired fidelity of the propagation model.

Multi layered plasma Here, we separate the plasma into many layers with the plasma density and background magnetic field *constant* in each layer. This allows us to solve the CPDR in each layer, and propagate the wave across layers by taking into account the reflection and refraction, through solution of Γ and T, and the boundary conditions at each interface. This solution method offers greater precision with increasing layers. Multiple reflections per layer can also be accommodated.

4.3 Remarks

Each of the techniques outlined above carries consequences on the field solution construction in general, and in terms of the mode polarization.

Incidentally, we are free to completely solve the Maxwell equations throughout the entire region. We would need a complete three dimensional characterization of the plasma structure, and a concomitant three dimensional solution to the equations in the entire region, which would depend on how we treated the inner and outer ionospheric boundaries. This is, however, an arduous task, and while not impossible, the boundary assumptions outlined above make field solutions much easier with no significant loss in accuracy in either realm.

At this point, we see that we have the necessary tools to solve for each mode's wave propagation by assuming a smooth boundary and using the ray tracing assumption, so we focus now on the correct method of solution for abrupt plasma boundaries. This involves solving for the reflection and transmission coefficients at an interface.

5 EM wave reflection and refraction at an abrupt interface

To find the transmission and reflection characteristics for each mode component of the EM wave we must assume an abrupt boundary and satisfy the boundary conditions at the interface. This situation is illustrated in Fig. 8. Here, the dielectric represented by refractive index $\boldsymbol{n_2}$ can represent a magnetized plasma with a complex value and tensor characteristics. For that case, the refracted wave number $\boldsymbol{k_t}$ would represent the superposition if the fast and slow mode CPDR solutions.

We are interested in the wave field components just inside the plasma boundary, so we assume a uniform plasma within which the orientation of the transmitted wave number and magnetic field, $\boldsymbol{k_t} \cdot \mathbf{B_0}$, does not change. This is analogous to dividing the plasma into many thin shells, except that we are only interested in the first shell. Gradients in $\boldsymbol{n_0}$ and $\mathbf{B_0}$ are accounted for in this manner by changing their values in each successive shell as necessary.

This case is essentially the first step in solving the wave propagation through a magnetized plasma divided into symmetric shells, accounting for reflection at each shell boundary. Here, we find the reflection and transmis-

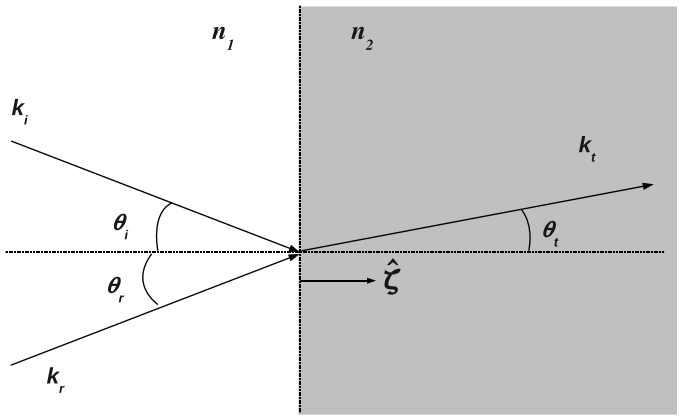

Figure 8: Geometry for an EM wave incident on a dielectric half space. The dielectric has refractive index $\boldsymbol{n_2}$, which can be complex.

sion coefficients (Γ and T respectively) for the wave field amplitudes at the boundary for each mode, and then multiply each spatial component of the wave field mode components by Γ and T for each mode (fast, or slow) to get their respective amplitudes.

5.1 Boundary conditions

Wave reflection and refraction at a plane interface is well understood, and can be described in terms of two general properties [5]:

Kinematic

These properties follow from the wave nature of the interaction and do not depend on the specific type of wave (acoustic, electromagnetic, etc.). The first is that the angle of reflection equal to the angle of incidence,

$$\theta_i = \theta_r \tag{46}$$

and the second is Snell's law:

$$\sin\theta_i / \sin\theta_t = n_t / n_i \tag{47}$$

where θ_i, θ_t are the angles of incidence and transmission with respect to the interface normal, and n_i, n_t are the indices of refraction in the medium of the incident and transmitted waves respectively.

Dynamic

These properties are completely dependent on the specific nature of the waves and their boundary conditions. For electromagnetic waves, they specify the behaviour of the tangential and normal fields across the interface. Specifically, the tangential components of $\boldsymbol{E}$ and $\boldsymbol{H}$ (where $\boldsymbol{H} = \boldsymbol{k} \times \boldsymbol{E}/\omega\mu$), thus the tangential components of $\boldsymbol{k}$, are continuous across the boundary

$$\begin{aligned} (\boldsymbol{E_i} + \boldsymbol{E_r} - \boldsymbol{E_t}) \times \hat{\boldsymbol{\xi}} &= 0 \\ \frac{1}{\mu_i}(\boldsymbol{k_i} \times \boldsymbol{E_i} + \boldsymbol{k_r} \times \boldsymbol{E_r} - \frac{1}{\mu_t}(\boldsymbol{k_t} \times \boldsymbol{E_t}) \times \hat{\boldsymbol{\xi}} &= 0 \end{aligned} \tag{48}$$

where $\hat{\boldsymbol{\xi}}$ is the unit normal to the interface and μ_i, μ_t are the permeabilities in the incident and transmitted wave media respectively ($\mu_i = \mu_t = \mu_0$ for our study).

The normal electromagnetic wave field components are continuous across the boundary only in the absence of any free charge at the interface. So, for instance, at the interface of two ideal dielectrics, the boundary conditions on those components would specify field continuity.

Ideal Dielectric

$$\begin{aligned} [\epsilon_i(\boldsymbol{E_i} + \boldsymbol{E_r}) - \epsilon_t \boldsymbol{E_t}] \cdot \hat{\boldsymbol{\xi}} &= 0 \\ [\boldsymbol{k_i} \times \boldsymbol{E_i} + \boldsymbol{k_r} \times \boldsymbol{E_r} - \boldsymbol{k_t} \times \boldsymbol{E_t}] \cdot \hat{\boldsymbol{\xi}} &= 0 \end{aligned} \tag{49}$$

where ϵ_i, ϵ_t represent the permittivity for the media of the incident and transmitted waves respectively. However, for an interface involving the presence of free charges such as a plasma, these field components will be discontinuous:

Free Surface Charge

$$\begin{aligned} [\epsilon_i(\boldsymbol{E_i} + \boldsymbol{E_r}) - \epsilon_t \boldsymbol{E_t}] \cdot \hat{\boldsymbol{\xi}} &= \rho_s \\ [\boldsymbol{k_i} \times \boldsymbol{E_i} + \boldsymbol{k_r} \times \boldsymbol{E_r} - \boldsymbol{k_t} \times \boldsymbol{E_t}] \cdot \hat{\boldsymbol{\xi}} &= \boldsymbol{J_s} \end{aligned} \tag{50}$$

The discontinuity is specified by a surface charge pileup ρ_s and surface current density $\boldsymbol{J_s}$ which are driven self consistently by the wave fields. These discontinuities, or jump conditions, are non-physical only in the sense that they are localized to an ideal interface described by an infinitesimally thin planar boundary surface. For example, there are finite scale lengths over which the plasma density gradient exists, over which the charge and current will distribute. Their localization to the zero thickness surface of the interface in this formalism is due to our assumption of an ideal boundary with zero thickness.

Note that calculation of the wave field components across a plasma boundary is completely specified using Snell's law as manifested by the continuity of the *tangential* field components (eqns. 47 and 48) [5]. This includes the field reflection and transmission coefficients given below.

Before we study the general case of oblique incidence of an electromagnetic wave on a plasma half space (bounded on the left by the x-y plane - see Fig. 9), we will review the results of the derivation of Γ and T for waves in free space incident on a dielectric half space [3, 4, 5] for principal orientations with respect to the incidence plane, summarizing the results. In terms of the incident wavenumber, we will review the results for an incident wave characterized by $\boldsymbol{k_i} = \boldsymbol{x}k_x + \boldsymbol{z}k_z$, and generalize to oblique incidence, where $\boldsymbol{k_i} = \boldsymbol{x}k_x + \boldsymbol{y}k_y + \boldsymbol{z}k_z$.

5.2 Field polarization nomenclature for field interaction at an interface

We will adopt the general nomenclature for labelling E-field components at an interface [5, 3, 4]. Referring to Fig. 8, the *plane of incidence* is defined as the plane formed by the surface normal vector $\hat{\boldsymbol{\xi}}$ and the incident wave number vector $\boldsymbol{k_i}$. E-field components *in* this plane are referred to as *parallel* polarized, and E-field components *perpendicular* of this plane are referred to as *perpendicular* polarized. This is different from magnetized plasma nomenclature, where parallel and perpendicular are usually referenced to the direction of the magnetic field $\mathbf{B_0}$.

5.3 Parallel incident electric field polarization

The electric field components of the incident wave that lie in the plane *perpendicular* to the interface plane (E_x and E_z for our case - see Fig. 10) are

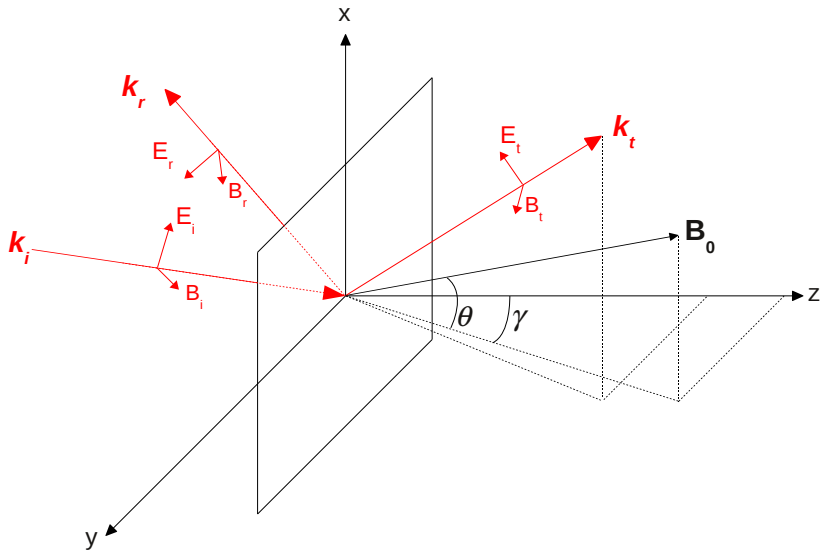

Figure 9: Geometry for an EM wave incident on a plasma half space. The plasma region is $\boldsymbol{z} > 0$.

specified across the plasma boundary, for each plasma mode (+ slow, - fast), with the reflection and transmission coefficients [5]

$$\begin{aligned} \Gamma_{||}(\pm) &= \frac{n_\pm^2 \cos\theta_i - (n_\pm^2 - \sin^2\theta_i)^{1/2}}{(n_\pm^2 - \sin^2\theta_i)^{1/2} + n_\pm^2 \cos\theta_i} \\ T_{||}(\pm) &= \frac{2n_\pm \cos\theta_i}{(n_\pm^2 - \sin^2\theta_i)^{1/2} + n_\pm^2 \cos\theta_i} \end{aligned} \tag{51}$$

where θ_i is the angle between the interface surface normal $\hat{\boldsymbol{\xi}}$ and the incoming wave number $\boldsymbol{k_i}$ in the interface ($\boldsymbol{x} - \boldsymbol{z}$ in this case) plane.

5.4 Perpendicular incident electric field polarization

The electric field components of the incident wave that lie *parallel* to the interface plane, or *perpendicular* to $\boldsymbol{k_i}$ in this plane (E_y for our case - see Fig. 11) are specified across the plasma boundary, for each plasma mode (+

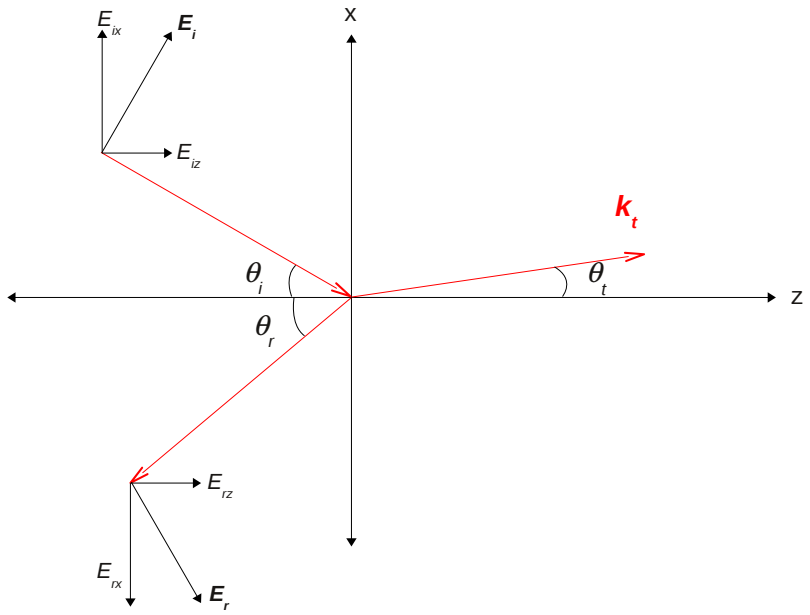

Figure 10: Parallel incident wave electric field polarization at a boundary in the $\boldsymbol{x}$-$\boldsymbol{y}$ plane.

slow, - fast), with the following reflection and transmission coefficients [5]

$$\begin{aligned} \Gamma_\perp(\pm) &= \frac{\cos\theta_i - (n_\pm^2 - \sin^2\theta_i)^{1/2}}{(n_\pm^2 - \sin^2\theta_i)^{1/2} + \cos\theta_i} \\ T_\perp(\pm) &= \frac{2\cos\theta_i}{(n_\pm^2 - \sin^2\theta_i)^{1/2} + \cos\theta_i} \end{aligned} \tag{52}$$

with θ_i specified as above. In the above equations for Γ and T for each incident wave field polarization, we have substituted the plasma refractive index for slow and fast modes, $n_\pm$, for the second medium. We can do this as long as the wave number is properly solved in the plasma when we calculate the plasma refractive index $n_\pm^2 = c^2/\omega^2\ k_\pm^2$ in the CPDR.

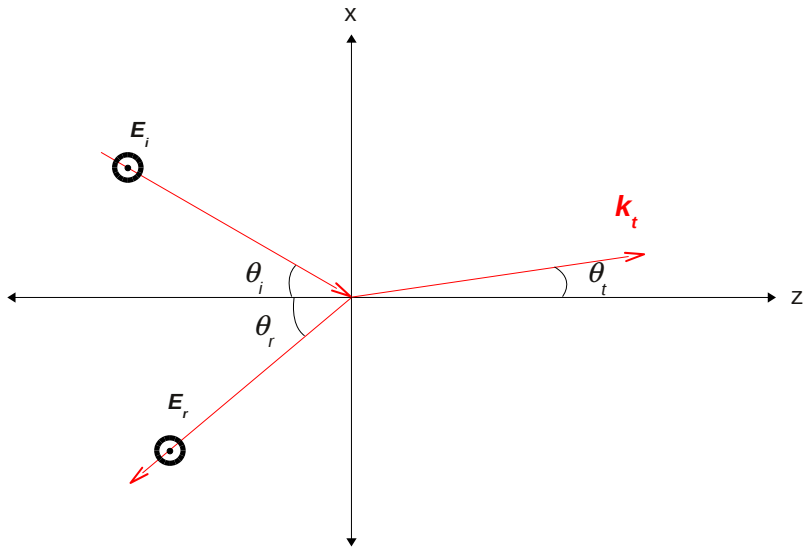

Figure 11: Perpendicular incident wave electric field polarization at a boundary in the $\boldsymbol{x}$-$\boldsymbol{y}$ plane.

5.5 Oblique incidence - arbitrary electric field polarization

In the previous two sections, we reviewed the reflection and transmission coefficients for the two possible electric field polarizations with respect to the plane of incidence: the plane formed by the normal to the plasma interface and the incident wavenumber $\boldsymbol{k_i}$. This happened to be the x-z plane for our example, and $\boldsymbol{k_i}$ was specified with only x and z components. We now generalize the situation to oblique incidence, where $\boldsymbol{k_i}$ can have components in all three directions (as in figs. 2 and 9). The vacuum/plasma interface is specified as the x-y plane, as before. However, care must be taken in choosing the incidence plane, as it will dictate which electric field polarization is necessary when calculating Γ and T.

Consider an incident wave as shown in Figs. 12 and 13. It approaches from below the y-z plane and in front of the x-z plane, and reflects behind the x-z plane and above the y-z plane. The electric field associated with this wave can have components in all three directions. We can choose the plane of incidence (different from the *interface* plane, as outlined above) to be either the x-z or y-z plane.

y-z plane

This configuration is shown in Fig. 12. E_x is perpendicular, and E_y, E_z are parallel to the incidence plane. $\Gamma(\perp, \parallel)$ and $T(\perp, \parallel)$ are calculated using the incidence angle θ_{yz}, found from the projection of the incident and reflected wavenumbers in the y-z plane.

x-z plane

This configuration is shown in Fig. 13. E_y is perpendicular, and E_x, E_z are parallel to the incidence plane. $\Gamma(\perp, \parallel)$ and $T(\perp, \parallel)$ are calculated using the incidence angle θ_{xz}, found from the projection of the incident and reflected wavenumbers in the x-z plane.

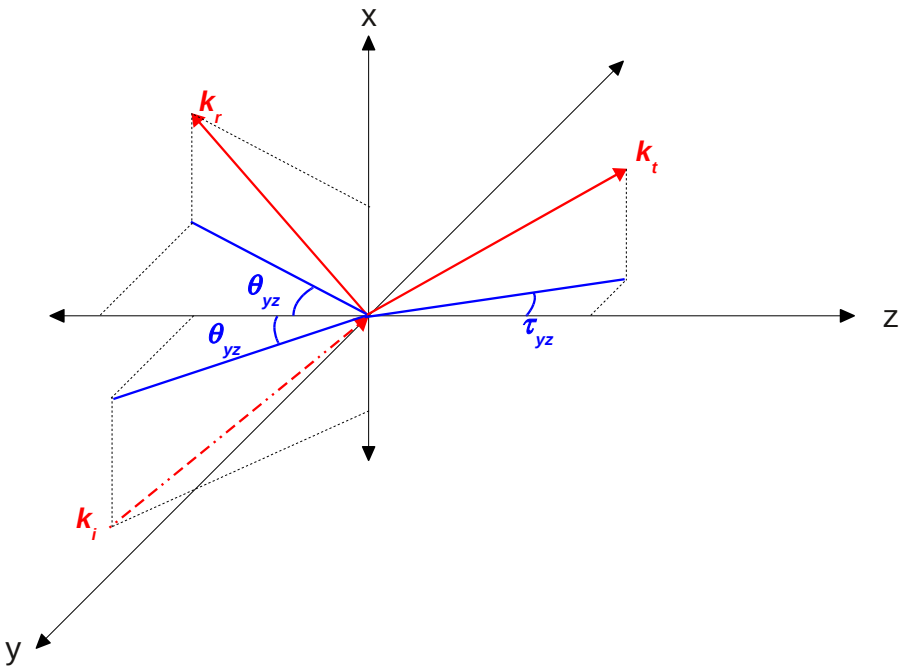

Figure 12: Oblique incidence at the plasma/vacuum interface. Choosing the y-z plane as the incidence plane.

We are free to choose the incidence plane for oblique incidence; the calculation of the reflected and transmitted field components will be unaffected as long as the proper polarization and corresponding angle of incidence are used.

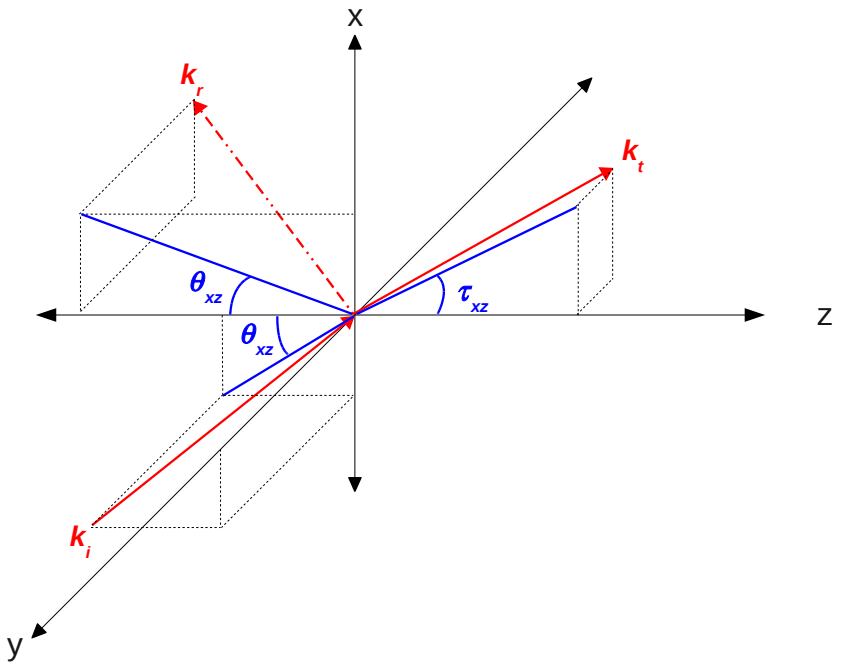

Figure 13: Oblique incidence at the plasma/vacuum interface. Choosing the x-z plane as the incidence plane.

Note that we have been concerned with the calculation of the wave field electric (and magnetic through Maxwell's equations) components in both media. Calculation of the transmitted wavenumber is done using the CPDR, shown below.

5.6 Wave field components - mode contribution

The reflected and transmitted wave electric field components can now be found for each mode using equations 51 and 52 with either n_+ or n_-.

$$E_j^{\boldsymbol{r,F/S}} = \Gamma_\kappa^{\mathbf{F/S}} E_j^{\boldsymbol{i,F/S}} \qquad E_j^{\boldsymbol{t,F/S}} = T_\kappa^{\mathbf{F/S}} E_j^{\boldsymbol{i,F/S}} \tag{53}$$

where j can be x, y or z corresponding to the field component and the superscripts **i, r, t** signify incident, reflected, and transmitted components respectively. The particular transmission and reflection coefficient polarization is represented by κ, and can be either parallel $\parallel$ or perpendicular $\perp$ depending on the chosen plane of incidence as outlined in section 5.5. The

incident field is a vacuum solution to Maxwell's equations, which we have separated into fast and slow components using the mode polarization unit vector $\hat{\boldsymbol{Q}}^{\boldsymbol{F/S}}$ from equation 42,

$$\begin{aligned} E_j^{\boldsymbol{r,F}} &= \mathit{\Gamma}_\kappa^{\mathbf{F}} \left(\boldsymbol{E_{inc}} \cdot \hat{Q}_j^F \right) \\ E_j^{\boldsymbol{r,S}} &= \mathit{\Gamma}_\kappa^{\mathbf{S}} \left(\boldsymbol{E_{inc}} \cdot \hat{Q}_j^S \right) \\ E_j^{\boldsymbol{t,F}} &= T_\kappa^{\mathbf{F}} \left(\boldsymbol{E_{inc}} \cdot \hat{Q}_j^F \right) \\ E_j^{\boldsymbol{t,S}} &= T_\kappa^{\mathbf{S}} \left(\boldsymbol{E_{inc}} \cdot \hat{Q}_j^S \right) \end{aligned} \tag{54}$$

The wave magnetic fields are found from Faraday's equation

$$\mathbf{H^{i/r/t,F/S}} = \frac{1}{\omega \mu_0} \boldsymbol{k} \times \mathbf{E^{i/r/t,F/S}} \tag{55}$$

5.6.1 Remarks

We now have the tools necessary to calculate the transmitted and reflected fields for each mode at an abrupt plasma boundary. However, in order to carry them out, we need to solve the magnitude of the plasma index of refraction for each mode and substitute that in $\Gamma^{F/S}, \mathrm{T}^{F/S}$, and $\hat{\boldsymbol{Q}}^{\boldsymbol{F/S}}$.

5.7 Solving the plasma index of refraction

The solutions for $\Gamma^{F/S}, \mathrm{T}^{F/S}$, and $\hat{\boldsymbol{Q}}^{\boldsymbol{F/S}}$, from equations 51, 52, and 41 respectively, involve the index of refraction. And, as pointed out earlier, the solution for its magnitude, where $\pm$ denotes slow/fast modes respectively,

$$|\boldsymbol{n}_\pm| = n_\pm = (c/\omega)|\boldsymbol{k}_\pm| \tag{56}$$

is independent of coordinate transforms up to three dimensions. So we are free to solve for it in any coordinate system we choose. However, we must do this by satisfying the boundary conditions on $k_\pm$ at the plasma interface. The boundary condition on the wave vector is that the incident tangential component at the boundary, $k_{i,tan}$, must equal the tangential component of the wave vector in the plasma ,$k_{\pm,tan}$ in *the same coordinate system.* This is best accomplished by preserving the tangential wave vector across the boundary

in the *original* coordinate system, which is where the actual boundary was specified.

The dispersion relation is found from equation 10

$$\det \begin{vmatrix} \epsilon'''_{11} - (n_y^2 + n_z^2) & \epsilon'''_{12} + n_x n_y & \epsilon'''_{13} + n_x n_z \\ \epsilon'''_{21} + n_x n_y & \epsilon'''_{22} - (n_x^2 + n_z^2) & \epsilon'''_{23} + n_y n_z \\ \epsilon'''_{31} + n_x n_z & \epsilon'''_{32} + n_y n_z & \epsilon'''_{33} - (n_x^2 + n_y^2) \end{vmatrix} = 0 \qquad (57)$$

with the plasma dielectric tensor rotated in from the symmetric coordinate system as outlined in section 2.2.2

$$\overline{\epsilon'''_{\mathbf{r}}} = \overline{\mathbf{R}}^{\mathbf{T}} \cdot \overline{\epsilon_{\mathbf{r}}} \cdot \overline{\mathbf{R}} \qquad (58)$$

In this coordinate system (original), with respect to the plane of incidence, we preserve the tangential components of $\mathbf{n}$ and solve for the perpendicular component. We originally specified a plasma half-space problem, with the interface between plasma and vacuum being the x-y plane, as illustrated in Fig. 9, and therefore we are solving for $n_{z,\pm}$ with $n_{x,\pm}$ and $n_{y,\pm}$ given by their vacuum values.

Once we have computed $n_{z,\pm}$, we can then substitute the appropriate fast/slow mode plasma index of refraction

$$|\boldsymbol{n}_{\pm}| = n_{\pm} = \sqrt{n_{x,\pm}^2 + n_{y,\pm}^2 + n_{z,\pm}^2} \qquad (59)$$

into $\Gamma^{F/S}$ and $\mathrm{T}^{F/S}$, from equations 51 or 52, and proceed to calculate the desired wave fields as in equations 54 and 55.

5.8 Poynting flux conservation at the boundary

We must choose the proper root (for each mode) in order to satisfy wave energy conservation as it crosses the boundary. This constraint is given by the conservation of the Poynting power flux; that is, the sum of the transmitted and reflected components of the EM wave power must equal its incident power. Computationally, as a result of some of the assumptions that can be made, this criterion can not be met for all cases, as described below. Furthermore, thermal and damping effects are, by definition, neglected in our calculation due to the assumption of a cold, collisionless plasma, which dictated the specific form of the plasma dielectric tensor used throughout (Eq. 11). These, as well as mode conversion and non-linear effects can be

treated by using the appropriate form of the plasma dielectric tensor, and concomitant technique, in solving the CPDR; but this is beyond the scope of the current report. However, in the VHF frequency bandwidth, the cold plasma assumption is appropriate for the majority of field calculations.

5.8.1 Smooth (gradual) transition

The assumptions outlined earlier regarding field propagation calculations for a gradual boundary, that is the ray tracing limit, neglect the correct treatment of wave reflections. The reflected wave component is dropped, or insufficiently treated, to the extent that the sum of transmitted and reflected powers will not equal the incident power. The completely rigorous method of including reflections at a gradual boundary is to resort to a full wave solution of Maxwell's equations in the entire region - which can be tedious and time intensive. Fortunately, the ray tracing technique does not suffer from comparatively large differences in Poynting flux conservation, compared to those cases where reflections are included, for most situations of interest in the VHF frequency band. The definition of 'comparatively large', however, is determined for each specific calculation based on the desired accuracy, and can lead to incorrect results. The point is that reflections are not properly treated under the ray tracing approximation, and this must be taken into account.

We must still choose the proper root for each mode, and this is determined by the Poynting energy flux direction and behavior at large distances from the boundary. The power flux perpendicular to the boundary interface must flow from the incident side to the transmitted side if the mode is not cutoff or resonant on the transmitted side, and that power must go to zero at long distances away from the boundary on the transmitted side. If the mode does experience a cutoff on the transmitted side, the correct root for n_z (or that component perpendicular to the interface boundary) travels from the transmitted side to the incident side with the power at long distances from the boundary, on the transmitted side, going to zero - like a reflected component.

5.8.2 Abrupt boundary

As outlined earlier, in this formalism the boundary is treated as an ideal interface between two media - for example vacuum and dielectric. Here, we

can apply Poynting flux conservation in a straightforward manner. In calculating the transmission and reflection coefficients, T and Γ, at a boundary, we satisfy the boundary conditions on the tangential field components; that is, that they are preserved across the boundary. This gives the tangential fields on the transmitted side. With T and Γ we then find the tangential transmitted and reflected fields on the incident side. This information gives us a complete picture of the Poynting flux on both sides, in the direction *perpendicular* to the interface plane

$$\boldsymbol{P}_t + \boldsymbol{P}_r = \boldsymbol{P}_i \tag{60}$$

where the subscripts t, r, and i represent transmitted, reflected, and incident respectively. The fluxes in the above equation are found from the field expressions calculated with the help of the transmission and reflection coefficients.

The harmonic form of the fields given in equation 2 and the definition of the Poynting flux give

$$\boldsymbol{P}_\perp = \frac{1}{2}\mathrm{Re}\{\boldsymbol{E}_\parallel \times \boldsymbol{H}_\parallel^*\} \tag{61}$$

where the subscripts refer to the orientation of the quantities relative to the *interface plane*. From Faraday's Law

$$\nabla \times \boldsymbol{E} = -\frac{\partial \boldsymbol{B}}{\partial t} \tag{62}$$

we have

$$\boldsymbol{k} \times \boldsymbol{E} = \omega\mu_0 \boldsymbol{H} \Rightarrow E \sim \frac{\omega\mu_0}{k} H \tag{63}$$

Defining the *wave impedance* η as

$$\eta = \frac{\omega\mu_0}{k} \tag{64}$$

(in vacuum, $\eta_0 = 377$) equation 61 becomes

$$\boldsymbol{P}_\perp = \frac{1}{2}\mathrm{Re}\left\{\frac{\boldsymbol{E}_\parallel \boldsymbol{E}_\parallel^*}{\eta^*}\right\} \tag{65}$$

and we allow for the complex nature of η in a plasma medium (that is, k can be complex) by taking its complex conjugate in the above equation.

Equation 65 can now be used in Eq. 60 with Eq. 54 to verify Poynting flux conservation.

If a mode does experience a cutoff or resonance on the transmitted side, we still need to choose the correct root for n_z (or that component perpendicular to the interface boundary) since the *reflected* field on the incident side will be determined by Γ, and it must be calculated using the proper plasma refractive index root in equations 51 and 52.

6 Summary

An EM wave travelling across a plasma boundary, like a signal generated at the surface of the earth and travelling upward to space, will undergo birefringence due to the dispersive characteristics of the magnetized plasma in the ionosphere. This birefringence manifests as a mode splitting in the propagating EM wave; that is, the *single* root solution to Maxwell's equations in vacuum (where the one root comprises a forward and backward travelling wave) will split into a *double* root solution to Maxwell's equations in a magnetized plasma background. Each of these wave roots, identified as either the *fast* or *slow*, can propagate, be cutoff, or experience a resonance on the plasma side of the boundary; being partially or completely reflected at the interface. Once these modes have traversed the ionosphere, they must be superposed on the topside in order to solve for the wave propagation characteristics. We have presented a method to calculate the correct partitioning of a propagating EM wave as it traverses a magnetized plasma, as well as the reflection and transmission coefficients, in the framework of the two mode solution, at a plasma boundary.

In modelling EM wave propagation across a plasma boundary, we are free to choose the type of boundary and plasma inhomogeneity, depending on the desired model fidelity and computation time. However, without resorting to a full wave solution, the possibility of significant signal reflection from a plasma boundary dictates that more accurate results are attained using a many layered plasma model, accounting for reflection and transmission at each layer.

References

[1] W. P. Allis, S. J. Buchsbaum, and A. Bers. *Waves in Anisotropic Plasmas*. M. I. T. Press, 1963.

[2] K. G. Budden. *The Propagation of Radio Waves*. Cambridge University Press, 1985.

[3] R. E. Collin. *Foundations for Microwave Engineering*. McGraw-Hill, 1966.

[4] R. F. Harrington. *Time-Harmonic Electromagnetic Fields*. McGraw-Hill, 1961.

[5] J. D. Jackson. *Classical Electrodynamics*. Wiley, second edition, 1975.

[6] J. D. Kraus. *Radio Astronomy*. Cygnus-Quasar, second edition, 1986.

[7] T. H. Stix. *Waves in Plasmas*. Springer, second edition, 1992.

[8] D. G. Swanson. *Plasma Waves*. Institute of Physics, second edition, 2003.